ASD-TDR-63-236

The High Temperature Hypersonic Gasdynamics Facility—Mach Number 4 Operation

Paul Czysz

TECHNICAL DOCUMENTARY REPORT NO. ASD-TDR-63-236
May 1963

Directorate of Engineering Test
Deputy for Test and Support
Aeronautical Systems Division
Air Force Systems Command
Wright-Patterson Air Force Base, Ohio

Project No. 1426, Task No. 142601

NOTICES

FOREWORD

This report was prepared by Paul Czysz of the Hypersonic Gasdynamics Branch, Aerodynamics Division, Directorate of Engineering Test, Deputy for Test and Support, Aeronautical Systems Division, Wright-Patterson Air Force Base, Ohio. It describes the High Temperature Hypersonic Gasdynamics Facility, discusses calibration and research programs performed, and specific operating problems. The work covers the period from August 1961 through May 1962.

The development of the High Temperature Hypersonic Gasdynamics Facility is being pursued under the continuing Task number 142601, "Hypersonic Tunnel Studies" of Project 1426 "Experimental Simulation of Flight Mechanics."

The major portion of this report was prepared by Major Robert W. Milling whose reassignment prevented his completion of the report. The author wishes to acknowledge the significant contribution Major Milling made to this report.

ABSTRACT

The High Temperature, Hypersonic Gasdynamics Facility was developed as a result of the efforts of the Aeronautical Systems Division to extend the state-of-the-art in hypersonic aerodynamics simulation. The High Temperature Facility is an operational hypersonic wind tunnel supplied by high pressure, heated air from a zirconium oxide pebble heater. The maximum stagnation pressure is 40 atmospheres, and the maximum temperature is 4700°R. The facility is one of four of its kind in this hemisphere and the only Air Force facility of its type. This report describes its operation from August 1961 until May 1962 as a Mach 4 aerodynamic test facility. The successful operation of this facility is a significant achievement in the area of hypersonic aerodynamic testing techniques.

This technical documentary report has been reviewed and is approved.

Webster W Plourd
WEBSTER W. PLOURD
Colonel, USAF
Asst Deputy for Test and Support

PREPARED BY:

Paul Czysz
PAUL CZYSZ
Acting Chief, Hypersonic
Gasdynamics Branch
Aerodynamics Division

CONCURRED IN:

for Carl E Reichert
WILLIAM J. DuBOIS
Colonel, USAF
Acting Director of Engineering Test
Deputy for Test and Support

CONCURRED IN:

Hugh S. Lippman
HUGH S. LIPPMAN
Technical Director
Deputy for Test and Support

APPROVED BY:

Webster W Plourd
WEBSTER W. PLOURD
Colonel, USAF
Asst Deputy for Test and Support

TABLE OF CONTENTS

LIST OF ILLUSTRATIONS

TABLES

SYMBOLS

a	speed of sound $\frac{ft}{sec}$
A	area in.^{2}
d	diameter in.
g	acceleration of gravity 32.174 $\frac{ft}{sec^2}$
h	enthalpy $\frac{BTU}{lb}$
M	Mach number
p	pressure psia
Re/l	Reynolds number per foot, $\frac{\rho_\infty V_\infty}{\mu_\infty}$, $\frac{1}{ft}$
T	temperature °R
q	dynamic pressure psia
V	velocity $\frac{ft}{sec}$
X	Distance From Nozzle Exit, Positive Downstream From Exit. In.
α	correction to pressure ratio for real gas $\frac{(P/P_0)\text{ thermally perfect}}{(P/P_0)\text{ perfect}}$
β	correction to temperature ratio for real gas $\frac{(T/T_0)\text{ thermally perfect}}{(T/T_0)\text{ perfect}}$
γ	ratio of specific heats

SUBSCRIPTS

*	critical, M = 1
o	stagnation
2	behind normal shock
∞	free stream static condition

INTRODUCTION

The second hot cycle of operation of the ASD High Temperature Hypersonic Gasdynamics Facility was completed on 4 May 1962. Since the initiation of the cycle on 1 August 1961, 261 runs were made at a nominal Mach number of 4 at facility stagnation pressures up to 600 psig and stagnation temperatures approaching 4700°R. Eight major test programs were completed as were flow calibration studies. This report includes a discussion of operating problems, results of calibration tests, and findings of several of the test programs.

DESCRIPTION

The HTF is a blowdown wind tunnel operating at a nominal Mach number of 4 with an axisymmetric nozzle of 5-inch exit diameter. The test section is a free jet enclosed in a plenum tank which is equipped with an auxiliary pressure control so that the ratio of plenum pressure to the static pressure at the nozzle exit is approximately one. The models are mounted on a rotary model support capable of sequentially injecting up to six models into the flow for specific time intervals as controlled by an intervalometer. The test section flow exhausts to atmosphere through a supersonic diffuser.

Air for blowdown operation is stored in a tank farm at 80 atmospheres pressure. Running times of 5 to 10 minutes are common, while runs of 20 minutes duration have been made. A more complete description of the facility operation is given in reference 1.

The heart of the HTF is the storage heater consisting of a pressure vessel insulated with refractory brick which houses a zirconia pebble bed. By heating the bed from the top with a combustion burner a source of heat is available to heat air which, during the run, is fed to the bottom of the heater. A schematic arrangement of the system is shown in figure 1 and a general arrangement is shown in figure 9.

OPERATION

The flow rates presented in the first report concerning the HTF operation (reference 1) did not include the effect of dissociated products of combustion on flame temperature. Reference 3 gives the results of a study analyzing the flame temperature, and heat release for a propane, oxygen, air mixture including dissociated products of combustion. Based on this study, the flow rates of air, oxygen, and propane for burner operation are given in tables 1 and 2. Since the products of combustion leave the heater at a relatively low temperature, less than 1000°F, it was assumed that the energy associated with the dissociated products of combustion is available to heat the pebble bed.

Manuscript released by the author March 1963 for publication as an ASD Technical Documentary Report.

CALIBRATION

The nozzles used for the Mach 4 configuration of the facility were axisymmetric with an exit diameter of 5 inches. The contoured nozzle was designed using the Foelsch method modified to correct for tangent deviation at the exit and also corrected for boundary layer growth. The conical nozzles had approximately the same exit and throat dimensions as the contoured nozzle but were formed by a conical section with a 6°57' half-angle. A drawing of these two nozzles is shown in figures 6 and 7 and a table of coordinates for the contoured nozzle in table 3. The calibration was performed with a water-cooled pitot probe and an uncooled four-tube rake. Sketches of these devices are shown in figures 10 and 11. The complete survey of the flow for the contoured nozzle was performed with the pitot probe while the conical nozzle was surveyed on the centerline with the pitot probe, and the off centerline surveyed with the four-tube rake. The Mach numbers were computed using a table look-up procedure, correcting for real gas effects. The data obtained for each location was represented as a function of temperature by means of a least mean square curve fit for a second order polynominal. Each curve fit was a result of at least 100 individual data points; the maximum deviation of the data points from the curve was ± 1 percent. The coefficient for the equations representing the data are as follows:

MACH NUMBER AS A FUNCTION OF STAGNATION TEMPERATURE

TEST SECTION STATION			a_o	a_1	a_2
X	Y	Z			
0.00	0	0	4.354	-8569×10^{4}	$-.5355 \times 10^{6}$
0.50	0	0	4.537	$-.1695 \times 10^{3}$	$+.8271 \times 10^{6}$
1.00	0	0	4.842	$-.3153 \times 10^{3}$	$+.3017 \times 10^{7}$
1.50	0	0	4.792	$-.2594 \times 10^{3}$	$+.2207 \times 10^{7}$
2.00	0	0	4.907	$-.2952 \times 10^{3}$	$+.2725 \times 10^{7}$
2.50	0	0	5.075	$-.3612 \times 10^{3}$	$+.3683 \times 10^{7}$
3.00	0	0	4.958	$-.2519 \times 10^{3}$	$+.1879 \times 10^{7}$

$$M = a_o + a_1 T_o + a_2 T_o^2$$

MACH NUMBER AS A FUNCTION OF TEST SECTION STATION

STAGNATION TEMPERATURE	b_o	b_1	b_2
2500°R	4.106	$+1.295 \times 10^{-1}$	-5.312×10^{-3}
3000	4.044	$+1.152 \times 10^{-1}$	-2.506×10^{-3}
3500	3.988	$+1.192 \times 10^{-1}$	-4.306×10^{-3}
4000	3.925	$+1.281 \times 10^{-1}$	-6.935×10^{-3}
4500	3.860	$+1.823 \times 10^{-1}$	-2.173×10^{-3}

$$M = b_o + b_1 x + b_2 x^2$$

The Mach number distributions for both the conical and contoured nozzles in x and y directions is shown in figures 3 and 4, respectively. Both nozzles produced about the same axial gradients but gave surprisingly different Mach number profiles across the stream. Although the contoured nozzle gave poorer results, they are not considered too bad since this is a first attempt at a contoured nozzle with a varying free stream γ.

The data was compared to theoretical calculations for the performance of the nozzle based on a calorically imperfect, thermally perfect gas (reference 4) and boundary layer growth from reference 5. In figure 2 the comparison is presented for the exit Mach number as a function of stagnation temperature. Based on the correlation of the calibration data and the theoretical prediction, the performance envelope for the conical Mach 4 nozzle is shown in figure 9. The contoured nozzle is not presented since no major programs were run using this nozzle. All of the aerodynamic investigations reported in references 6 through 22 were performed using the conical nozzle.

STAGNATION TEMPERATURE DETERMINATION

The method of obtaining the stagnation temperature was somewhat unconventional. The highest temperature for which direct measurement was made with a thermocouple, was about 3000°F. Since the facility has an operating temperature considerably above this, a different method has been employed. An optical or radiation pyrometer could not be used since both theory (reference 2) and experiment showed a difference between air and matrix temperature at large weight flows. The facility was equipped to measure the stagnation pressure and total weight flow of air into the heater. The expression for nozzle weight flow is:

$$\dot{w} = \rho v a = \rho^* v^* A^* = \frac{P^* g\, A^*}{R\, T^*\, z^*} \sqrt{\gamma^* R\, z^* T}$$

This can be arranged to give:

$$\dot{w} = \frac{P_0}{\sqrt{T_0}} \frac{\alpha}{\sqrt{\beta}} \left[\frac{P^*}{P_0}\right]_{Perf} \cdot \left[\frac{T_0}{T^*}\right]_{Perf} \cdot \sqrt{\frac{\gamma^*}{RZ^*}} \cdot gA^*$$

for a calorically imperfect, thermally perfect gas $Z = 1$.

Rearranging we have

$$\frac{T_0}{A^{*2}} \frac{\beta}{\alpha^2 \gamma^*} = 0.2020 \left[\frac{P_0}{\dot{w}}\right]^2$$

Since the left side of the equation is only a function of temperature, the left side can be calculated as a function of temperature. The result is a linear relationship in the range $500 < to < 5000$°R.

$$T_0 = 0.26506\, A^{*2} \left[\frac{P_0}{w}\right]^2 + 62.5$$

OPERATING PROBLEMS

Any device used to produce high temperature air for hypersonic testing can be expected to have operating problems requiring the development of special operating techniques. The zirconia pebble-bed heater of the HTF is no exception and in fact, has presented many problems unique to the pebble-bed heater. Some of the major problems encountered will be discussed in this section and the techniques used to cope with these problems will be detailed.

During the previous operating cycle the method of slow initial heat-up was developed to minimize thermal stress in the refractory lining. While this was generally successful it was not sufficient to prevent eventual damage to the bricks in the dome area. As shown in figure 5, the bricks in the dome were in staggered rows so that each row carried the cantilevered load from the weight of the bricks above it. This load in combination with the thermal stress was sufficient in many cases to cause failure. To overcome this problem a new dome of different mechanical design was installed prior to the second cycle of operation. This design is similar to an igloo so that the loading is essentially compressive rather than bending (figure 5).

The inversion characteristic of zirconia is well known and is undoubtedly the greatest single disadvantage to using this material for heat storage. Since the hysteresis loop is centered about 1600-2100°F, cycling of some portion of the bed cannot be avoided. During the previous cycle the situation was aggravated by the use of air idling in which the top of the pebble bed dropped to as low as 1500°F, so that all of the zirconia was cycled through the inversion zone. It seemed obvious that the affected area could be minimized by increasing the minimum top-of-the-bed temperature to approximately 2500°F. However, obtaining this criteria requires that the burner be operated with oxygen enrichment during idle periods. Since the burner is less stable with oxygen enrichment it is more sensitive to mechanical fluctuations which caused some concern for the hazards of leaving the system unattended during idle periods. This method of idling was established even though it presented certain hazards to the operation of the facility. Of all the techniques developed it is believed that establishing a minimum top-of-the-bed temperature of 2500°F was the most important factor in extending the life of the refractories.

Although the top of the pebble bed can be maintained at 2500°F, the temperature at the interface is limited by temperature drop across the five feet of alumina pebbles above the supporting grate, which is normally limited to 1000°F temperature. After the operating cycle was completed in May 1962 and the refractory removed from the heater, the grate which was constructed of type 347 stainless steel was found to be severely warped and scaled. Analysis of the grate showed it had exceeded 1650°F. The thermocouple used to measure the grate temperature was placed in a well in contact with the grate. Since the discrepancy of this method was large; future installations will have the thermocouples attached directly to the grate. This also indicated that if the top of the bed was to be maintained at 2500°F, the grate would be overheated. To allow the zirconia to be at almost uniform temperature at approximately 2500°F for the idle condition, a side outlet for the combustion products has been installed (figure 6). This gives a five-foot-high column of alumina pebbles as an insulator for the grate. In order to avoid any reaction between the alumina and zirconia refractory, the interface temperature will be maintained between 2100° and 2300°F.

Operation of the burner with oxygen enrichment for long periods brought to light an additional problem which had not previously been considered. Because of a requirement related to the refractory material the burner is always operated oxygen rich; the products of combustion, therefore, contain both oxygen and nitrogen as well as large quantities of water vapor and possibly hydroxide. As the products of combustion pass out through the exhaust system they are cooled and at some point condensation occurs. While the exact chemistry of the process is unknown, the resulting condensate is a dilute solution of nitric acid. The piping at the bottom of the heater that is common to the combustion exhaust and the high pressure air supply had been thermally insulated to prevent condensation and no difficulty was encountered in this area. The remaining portion of the exhaust was severely damaged by corrosion from the nitric acid before the problem was recognized. Neutralization of the acid with ammonia was only partially successful since all the acid had not condensed at the point where the ammonia was injected. In the future a cooling coil will be inserted in the exhaust to condense all the condensible products of combustion at one location so that complete neutralization can be accomplished. In addition, stainless steel will be used for all future modifications on the exhaust system.

While raising the idle temperature provides a significant increase in refractory life it does not prevent cycling a portion of the pebble bed through the inversion zone during each test run of the facility. The inversion cycling causes the refractory material to fail by shearing action that produces dust which in turn causes the pebbles to adhere to one another. This process is called "clumping" which reduces the porosity of the pebble bed causing the pressure drop to increase. When the clump has become sufficiently large the pressure drop will be high enough to cause the bed to lift during a test run. This process, described in detail in reference 2, is generally referred to as bed flotation but this term is much too mild to describe the lifting which accompanies a large pebble clump. Regardless of the term used, when the bed lifts and pebbles are blown through the nozzle, it is a very serious condition that should be avoided.

In the past, a clump large enough to cause the bed to lift has been used to define the end of a cycle of heater operation. During this cycle, however, it was essential that a technique be developed to break up clumps without the necessity of cooling the heater. The technique employed was to lift the pebble bed intentionally by rapid pressurization of the heater. The procedure was to preset the flow modulating valve (valve MV-2 shown in figure 1) partially open and then pressurize the air supply line to the bottom of the heater by rapidly cycling the air supply valve, MV-1, repeatedly from closed to open to closed. The cycling of the air supply valve was quite repeatable so that the process could be controlled accurately by the preset opening of the modulating valve. With the top of the bed at 2500°F, lifting was computed to occur at about 13 psi pressure drop. During the "shaking" operation the measured pressure drop was compared to visual observations of the top of the bed. Significant lifts were obtained at 15 to 18 psid during the early stages of the cycle when clumping was apparently less severe; ten to twelve lifts were considered sufficient to break up the clump.

During the last weeks of operation clumping became very severe, to the extent that no general bed lifting was obtained until the pressure drop exceeded 30 psid. The exact pressure drop was not measured because it exceeded the range of the instrument. The pressure drop required for successive lifts decreased which indicated that the clump had been broken apart. After six or eight lifts the pressure required was normal; the operation was continued for a total of ten to twelve lifts. The height of the bed was increased appreciably during these lifts offering additional evidence that this technique was quite successful. The "shaking" operation, however, requires extreme care. The lifting must be sufficient to break up the clump but it must not be too high to cause pebbles to deposit on ledges or in the nozzle outlet from where they may roll out during a run.

CONCLUSIONS

The facility described herein provides the Air Force with the required in-house capability of a vigorous applied research program in aero-thermodynamics. It operates and meets the need of ASD in its demands for quick reaction capability in applied research. The HTF is not a "production" test facility in the sense of providing solutions to detail vehicle development problems. It is directed toward providing experimental verification and correlation of ideas in the detail that is required by the applied research engineer. For this reason, the life expectancy of any one configuration can be expected to be short. An experimental facility that does not keep pace with the advancing technology is of little use in applied research.

Construction is presently in progress on the extended Mach number range for the HTF. Since the stagnation temperature is limited to 4700°R it has been decided that little can be gained in presently going beyond Mach 14. The present facility is designed around a capability of 24-inch diameter axisymmetric nozzles at Mach 8, 10, 12, and 14. Procurement will be initiated later this year to extend this range further with a 16-inch diameter Mach 6, and a 19-inch diameter Mach 7 nozzle. Over the entire operating range from Mach 6 through Mach 14, a minimum constant Mach core of 10 inches diameter is available. Procurement is proceeding also for flow control and measuring system for the new Mach number range, a 50-channel pressure system with the range from 100 mm of Hg to approximately 50 μ of Hg, and a heat transfer system for 50 thermocouples. These instrumentation systems are scheduled for operational status at approximately the same time that the facility becomes operational.

The performance of this new system will be described in a future report.

REFERENCES

1. Milling, Robert W., Captain, USAF, "The High Temperature Hypersonic Gasdynamics Facility," ASD Technical Note 61-107, September 1961, ASTIA Document Nr 266 728.

2. Schumann, T. E. W., "Heat Transfer: A Liquid Flowing Through a Porous Prism," Journal of the Franklin Institute, Volume 208, 1929.

3. Czysz, Paul, "A Thermodynamic Study of the Air-Oxygen-Propane Burner for the High Temperature Facility," ASD Engineering Test Report, ASTEA 62-12R, 6 August 1962.

4. Ames Research Staff, "Equations, Tables, and Charts for Compressible Flow," NACA Report 1135, 1935.

5. Burke, A. F., "Turbulent Boundary Layer on Highly Cooled Surfaces at High Mach Numbers," Proceedings of Symposium on Aerothermoelasticity, pg 704-741, November 1961, ASD TR 61-645, ASTIA Document Nr 271 529.

6. Crook, Robert T., "Calibration of the HTF 5-Inch Contoured Nozzle - Flow Angularity and Centerline Mach Nr Distribution," ASD Engineering Test Report ASTEA 62-5R, 15 May 1962.

7. Crook, Robert T., "Operating Characteristics Investigation: High Temperature, Hypersonic Gasdynamics Facility," ASD Engineering Test Report ASTEA 61-24, 7 December 1961.

REFERENCES (CONT'D)

8. Crook, Robert T., "Calibration of the HTF 5-Inch Conical Nozzle," ASD Engineering Test Report, ASTEA 62-4R, 16 April 1962.

9. Crook, Robert T., "Experimental Verification of the Frictional Pressure Drop Through Porous Media," ASD Technical Note 61-119, October 1961. ASTIA Document Nr 269 484.

10. Crook, Robert T., "Thermantic Structural Composites Test," ASD Engineering Test Report, ASTEA 61-1R, 18 January 1962.

11. Czysz, Paul, "Correlation of Wind Tunnel Blockage Data," ASD TDR 63-230, February 1963.

12. Czysz, Paul, "Hemisphere Cylinder Heat Transfer Study," ASD TDR 63-404 February 1963.

13. Czysz, Paul, "Hypersonic Flow Photographs," ASD Engineering Test Report ASTEA 61-6R, 22 January 1962.

14. Czysz, Paul, "Effect of an Applied Electric Field on a Hypersonic Flow Field Around A Sphere," ASD Engineering Test Report, ASTEA 62-11R, 25 July 1962.

15. Czysz, Paul, "Preliminary Investigation of Ablation Nose Cones in the High Temperature, Hypersonic Gasdynamics Facility," ASD Engineering Test Report, WWFEA 61-14, 20 March 1961.

16. Czysz, Paul, "Investigation of Ablation Bodies in the High Temperature, Hypersonic Gasdynamics Facility," ASD Engineering Test Report ASTEA 62-2R, 8 February 1962.

17. Everling, Phillip C., "Aerodynamic Heating of a Blunted Cone with a Gas Ejecting Spike," ASD Engineering Test Report ASTEA 62-14R, 16 August 1962.

18. Smith, Richard R., "Investigation of Flow Variables on a Series of Rearward Facing Flat Plates," ASD TDR 63-131, January 1963.

19. Smith, Richard R., "Simulated Re-Entry Test," ASD Engineering Test Report, ASTEA 61-25, 11 December 1961.

20. DeCamp, R. W., Captain, USAF, (Unclas Title) "RAM (Radar Absorbent Material) Test," ASD TDR 63-

21. Burnett, Duane R., "Ramjet Combustion Studies," ASD TDR 63-196 February 1963.

22. Burnett, Duane R., "Hydrostatic Testing of Two High Pressure Air Storage Tanks of HTF," ASD Engineering Test Report, ASTEA 62-18R, 5 October 1962.

23. Cain, M. R., "Model Support System," ASD Engineering Test Report, ASTEA 62-9R, 31 July 1962.

APPENDIX I
RESUME OF EXPERIMENTAL PROGRAMS

Presented herein is a list of the accomplished experimental programs performed in the Mach 4 configuration of the HTF. Stated for each report is the objective and conclusions. A complete description of each program can be obtained from the original reports.

References 6 through 8 — Calibration Reports

Objective:

To determine the Mach number, and flow angularity as a function of stagnation pressure, stagnation temperature, and test section position.

Conclusions:

The Mach number could be determined as a function of stagnation temperature and test section position to within ± 1 percent. The effect of stagnation pressure was less than the uncertainty in the data. The flow angularity was hand calculated at several points and found to be very small, on the order of 1 degree maximum. Considering the static angle of attack was not repeatable to within 50 minutes, the flow angularity was virtually unmeasurable with the existing system.

Reference 9 — Experimental Verification of the Frictional Pressure Drop Through Porous Media

Objective:

To measure the frictional pressure drop across a porous bed, and verify the theory under easily controlled conditions; also to study the various phases of pebble motion within the bed, and the effect of the method of flow initiation on the frictional pressure drop of the bed.

Conclusions:

The theory gives slightly higher frictional pressure drop than those obtained for condition of the pebbles at rest, rolling, and shifting. There is excellent verification of the pressure drop required to fluidize the bed.

As weight flow and consequentially frictional pressure drop through a bed is increased, the pebbles at the top layers first spin or roll in place, during which the length of the bed remains approximately the same; it then begins shifting in the horizontal plane and finally it fluidizes with approximately the top one third of the bed lifting and then falling back repeatedly in a cyclic-like process.

The technique of flow initiation has an influence on the frictional pressure drop especially in the lower Reynolds range tested.

Reference 10 — Thermatic Structural Composite Test

Objective:

To determine the long term response of various structural panels to aerodynamic heating. The models were shapes constructed of ceramic honeycomb.

Conclusions:

Due to thermal shock failure of the ceramic, the metal honeycomb was exposed to the flow and model disintegration occurred in about 65 seconds instead of the programed 20 minutes.

Reference 11 – Correlation of Wind Tunnel Blockage Data

Objective:

To obtain the blockage limitation for the Mach 4 configuration of the facility and correlate the results with other investigators.

Conclusions:

Model blockage results can be reasonably well correlated as a function of Mach number and drag coefficient for most shapes even at angles of attack up to 40 degrees. The Sphere and Disk show the most scatter and although good correlation is not evident, the suggested permissible model size for $.8 < C_D < 2.0$ is not unreasonable considering the experimental results. The theory for predicting the maximum model size for slender bodies in an open test section is good. Therefore, the approximate maximum model which will start for both open and closed test section facilities can be established.

Reference 12 — Hemisphere Cylinder Heat Transfer Study

Objective:

To measure the stagnation point heat transfer of various-sized hemisphere-cylinder bodies and compare the results with various theories.

Conclusions:

The experimental heat transfer rates for the series of models from $R_0 = 0.30$ inches to a right circular cylinder can be correlated into a consistent set of data. An approximate method for estimating the stagnation point velocity gradient for a spherical segment was not contradicted by the data. The uncertainty and repeatability of the experimental data is no greater than ± 10 percent. This is no larger than the uncertainty associated with any particular theoretical estimate due to differences in values for the stagnation point velocity gradient and gas properties at the model surface. The heat transfer gauge used gave very good experimental results, and with improved quality control in installing the gauge, significant improvement in experimental accuracy should be possible.

Reference 13 –Hypersonic Flow Photographs

Objective:

To obtain schlieren photographs of the flow fields around several representative re-entry configurations.

Conclusions:

For models ejecting a gas whose density is significantly different than that of air, color schlieren techniques will show the path of the ejected gas.

Reference 14 –Effect of an Applied Electric Field on the Hypersonic Flow Field Around a Sphere

Objective:

To determine if visible radiation is produced by applying a high direct current voltage to an insulated sphere in a high temperature hypersonic air stream.

Conclusions:

Due to lag times associated with the readout equipment on the power supply, no real indications of the actual voltage applied to the model could be obtained. The material of the supporting strut ablated considerably and influenced the experiment, therefore, the exact nature and the extent to which the flow field was modified could not be determined.

References 15 and 16 – Investigation of Ablation Bodies

Objective:

To investigate relative gross heating and secondary heating areas by means of an ablating plastic material for a wide range of re-entry type bodies.

Conclusions:

The results indicate that this type test is not a good method for determining relative heating rates between a different configurations.

Reference 17 – Aerodynamic Heating of a Blunted Cone with a Gas Ejecting Spike

Objective:

To determine the effectiveness of a gas-ejecting nose spike in reducing the aerodynamic heating of a blunted cone afterbody up to 40-degree angle of attack.

Conclusions:

Comparison of the heat transfer rates show that the presence of the nose spike significantly increased the heat transfer rate to the afterbody, increasing the effect with increasing angle of attack. Ejecting a low molecular weight gas from the nose spike reduces the afterbody heat transfer but never to levels approaching the basic sphere-cone.

Reference 18 – Investigation of Flow Variables on a Series of Rearward Facing, Stepped Flat Plates

Objective:

To obtain experimental information on the aerodynamic characteristics of a flat plate with basic changes in the flow field imposed by geometric and aerodynamic means.

Conclusions:

The flat plate pressure distributions correlated well with established theories and other experimental data. The effect of leading edge bluntness, step height, and ejection angle, are small. While the effect of gas ejection is pronounced in the region close to the ejection nozzle, it is not sufficiently distributed to produce the effect of a physical control surface. The three dimensional losses were pronounced at high angles of attack.

References 19 and 20 – Radar Absorbent Materials Test

Objective:

To determine the manner in which a reinforced low density, polyurethane coating is lost from a surface during a range of environments which can be expected during ballistic re-entry and to determine whether the process would be detrimental to vehicle stability.

Conclusions:

The objective was accomplished with successful results.

Reference 21 – Ramjet Combustion Studies

Objective:

To develop diagnostic techniques for detection of hydrogen combustion in a hypersonic high temperature air stream.

Conclusions:

Supersonic hydrogen combustion in a hypersonic flow field can be detected by the following methods:

1. Photomultiplier tube sensitive at 3400 Å.
2. Infrared photography at wave lengths longer than 6300 Å.
3. Color, and Black and White film in visible spectral regions.
4. Pressure distribution over body.

Reference 22 Hydrostatic Testing of Two High Pressure Air Storage Tanks

Objective:

Determine number of cycles to failure of the Mark I torpedo flasks used to store air at 1200 psig for the High Temperature, Hypersonic Gasdynamics Facility.

Conclusions:

The cycling from 100 psig to 2000 psig for 1000 cycles, then from 100 psig to 4000 psig for 3 cycles, and a final pressurization to 5600 psig, produced no cracks, leaks, or other structural failure of the two randomly chosen flasks.

TABLE 1

FLOW RATES FOR BURNER OPERATION - AIR AND PROPANE

TEMP °R	2000	2200	2400	2600	2800	3000	3200	3400	3750
O_2/C_3H_8	14.8	12.8	11.1	9.82	8.75	7.89	7.18	6.57	5.56
N_2/C_3H_8	55.7	48.2	42.1	37.1	33.0	29.8	27.1	24.8	21.0
BTU/HR 1.25×10^{5}	3879 0.91	3358 0.91	2929 0.91	2581 0.91	2300 0.91	2073 0.91	1886 0.91	1724 0.91	1426 0.91
1.50×10^{5}	4655 1.09	4030 1.09	3515 1.09	3097 1.09	2760 1.09	2488 1.09	2263 1.09	2068 1.09	1754 1.09
1.75×10^{5}	5431 1.27	4701 1.27	4101 1.27	3616 1.27	3220 1.27	2902 1.27	2641 1.27	2413 1.27	2047 1.27
2.00×10^{5}	6207 1.45	5373 1.45	4687 1.45	4129 1.45	3680 1.45	3317 1.45	3018 1.45	2758 1.45	2339 1.45
3.00×10^{5}	9311 2.18	8059 2.18	7030 2.18	6194 2.18	5520 2.18	4976 2.18	4527 2.18	4137 2.18	3507 2.18
4.00×10^{5}		10750 2.90	9373 2.90	8258 2.90	7360 2.90	6634 2.90	6036 2.90	5516 2.90	4678 2.90
5.00×10^{5}				10323 3.63	9200 3.63	8293 3.63	7544 3.63	6895 3.63	5848 3.63
6.00×10^{5}						9951 4.35	9053 4.35	8274 4.35	7017 4.35
7.00×10^{5}							10560 5.08	9653 5.08	8187 5.08
8.00×10^{5}									9356 5.80
9.00×10^{5}									10530 6.53
1.00×10^{6}									11695 7.25

AIR FLOW RATE = SCFH
O_2 FLOW RATE = SCFM
C_3H_8 FLOW RATE = SCFM

TABLE 2

FLOW RATES FOR BURNER OPERATION - AIR, OXYGEN, AND PROPANE

TEMP °R	3400	3600	3800	4000	4200	4400	4600	4800	5000
O_2/C_3H_8	6.50	6.50	6.50	6.50	6.50	6.50	6.50	6.50	6.50
N_2/C_3H_8	24.6	22.0	19.4	16.9	14.5	12.1	9.66	7.22	4.74
BTU/HR 2.00x10^5	2743 0.0 1.45	2447 0.99 1.45	2162 1.99 1.45	1884 2.96 1.45	1613 3.91 1.45	1344 4.85 1.45	1076 5.78 1.45	804 6.73 1.45	527 AIR 7.70 O_2 1.45 C_3H
4.00x10^5	5487 0.0 2.90	4894 1.99 2.90	4323 3.98 2.90	3768 5.92 2.90	3225 7.82 2.90	2688 9.69 2.90	2151 11.6 2.90	1609 13.5 2.90	1055 15.6 2.90
5.00x10^5	6859 0.0 3.63	6118 2.48 3.63	5404 4.98 3.63	4710 7.40 3.63	4031 9.77 3.63	3360 12.1 3.63	2689 14.5 3.63	2011 16.8 3.63	1319 19.2 3.63
6.00x10^5	8230 0.0 4.35	7342 2.98 4.35	6485 5.97 4.35	5652 8.88 4.35	4838 11.7 4.35	4032 14.5 4.35	3227 17.3 4.35	2413 20.1 4.35	1582 23.1 4.35
7.00x10^5	9602 0.0 5.08	8565 3.48 5.08	7565 6.97 5.08	6595 10.4 5.08	5644 13.7 5.08	4704 17.0 5.08	3765 20.2 5.08	2816 23.5 5.08	1846 26.9 5.08
8.00x10^5		9789 3.98 5.80	8646 7.96 5.80	7537 11.8 5.80	6450 15.6 5.80	5376 19.4 5.80	4302 23.1 5.80	3218 26.9 5.80	2110 30.8 5.80
9.00x10^5			9727 8.96 6.53	8479 13.3 6.53	7256 1716 6.53	6048 21.81 6.53	4840 26.0 6.53	3620 30.3 6.53	2373 34.6 6.53
1.00x10^6				9421 14.8 7.25	8063 19.5 7.25	6720 24.2 7.25	5378 28.9 7.25	4022 33.6 7.25	2637 38.5 7.25
1.10x10^6					8869 21.5 7.98	7392 26.6 7.98	5916 31.1 7.98	4425 37.0 7.98	2901 42.3 7.98
1.20x10^6						8064 29.1 8.70	6453 34.7 8.70	4827 40.4 8.70	3164 46.2 8.70
1.4x10^6							7529 40.5 10.2	5631 47.1 10.2	3692 53.9 10.2

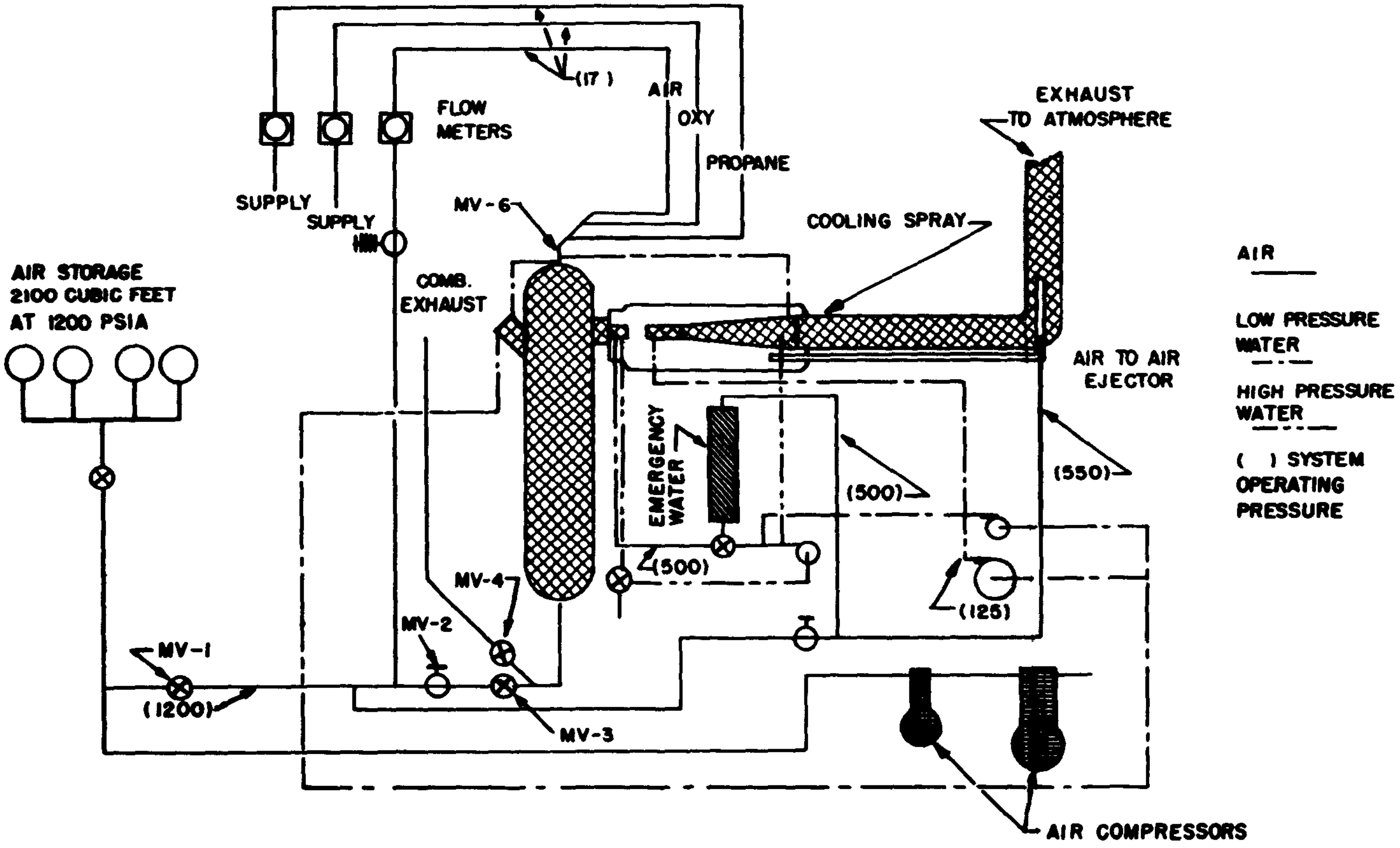

Figure 1. Schematic Arrangement of the High Temperature Facility

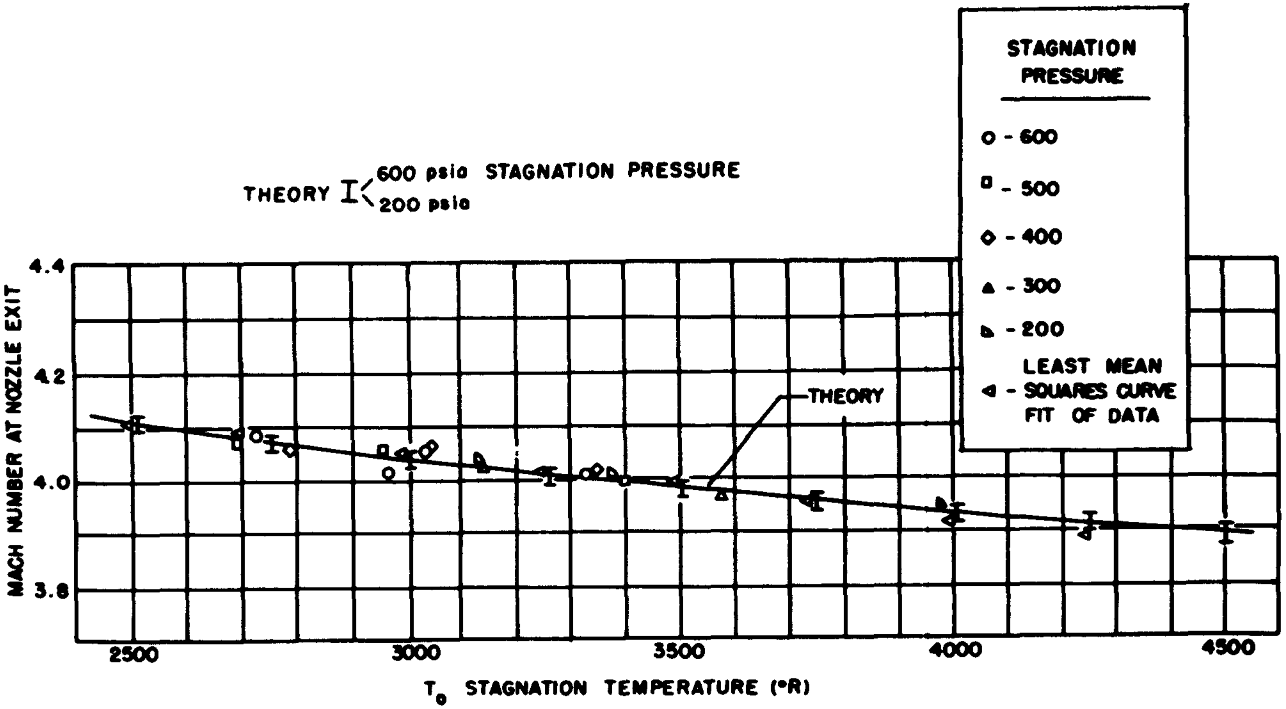

Figure 2. Comparison of Theoretical Estimate for the Conical Mach 4 Nozzle with Calibration Data

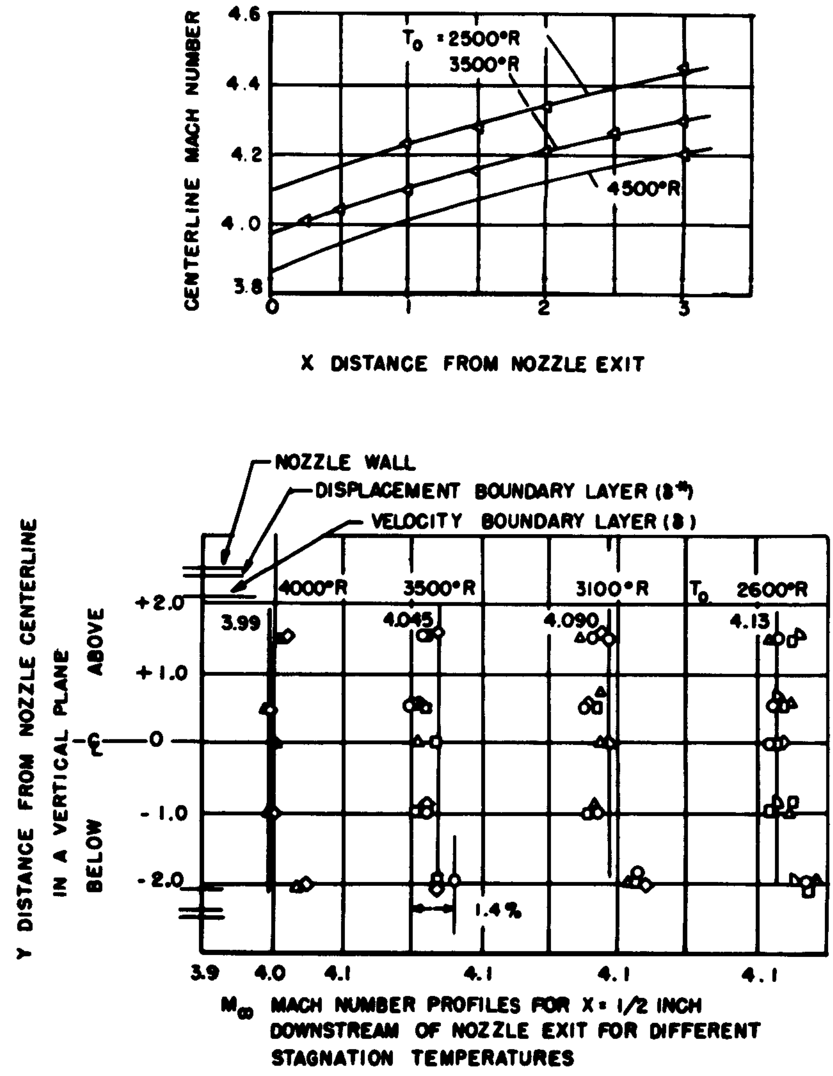
LEGEND THE SAME AS FOR FIGURE 2

Figure 3. Mach Number Profiles for the Conical Mach 4 Nozzle

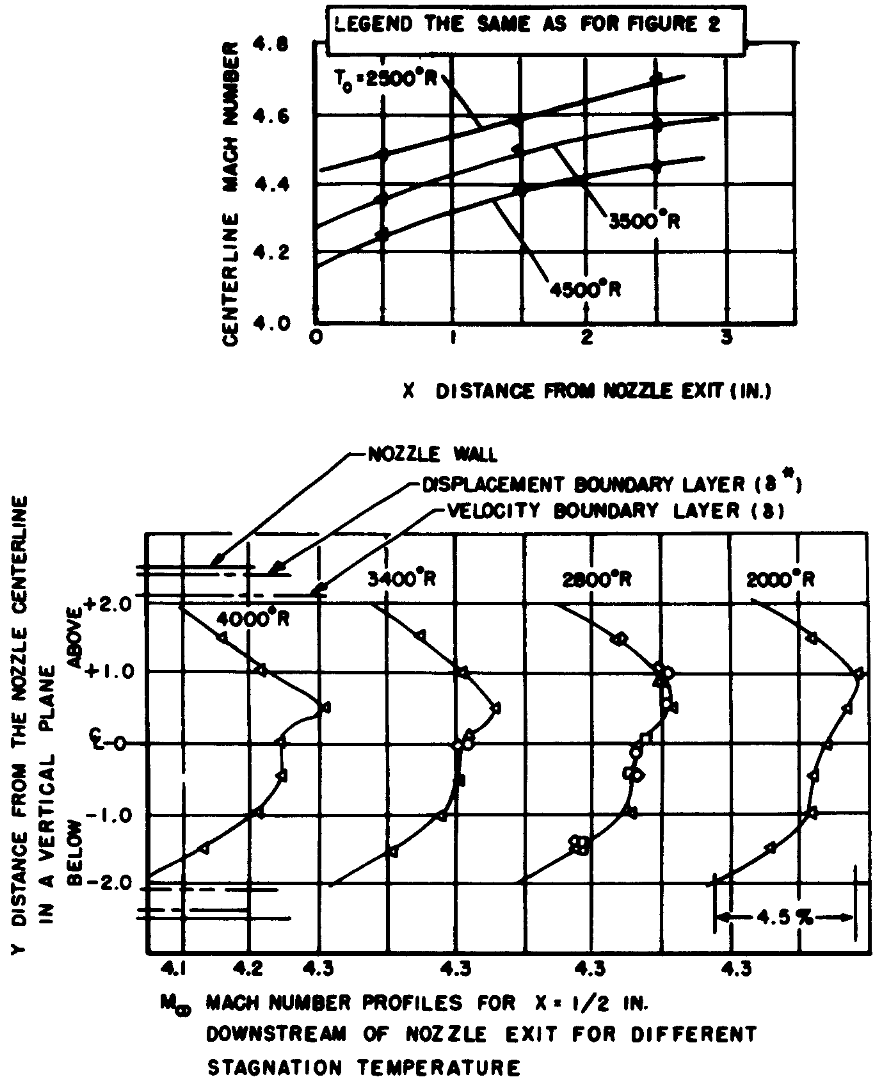

Figure 4. Mach Number Profiles for the Contoured Mach 4 Nozzle

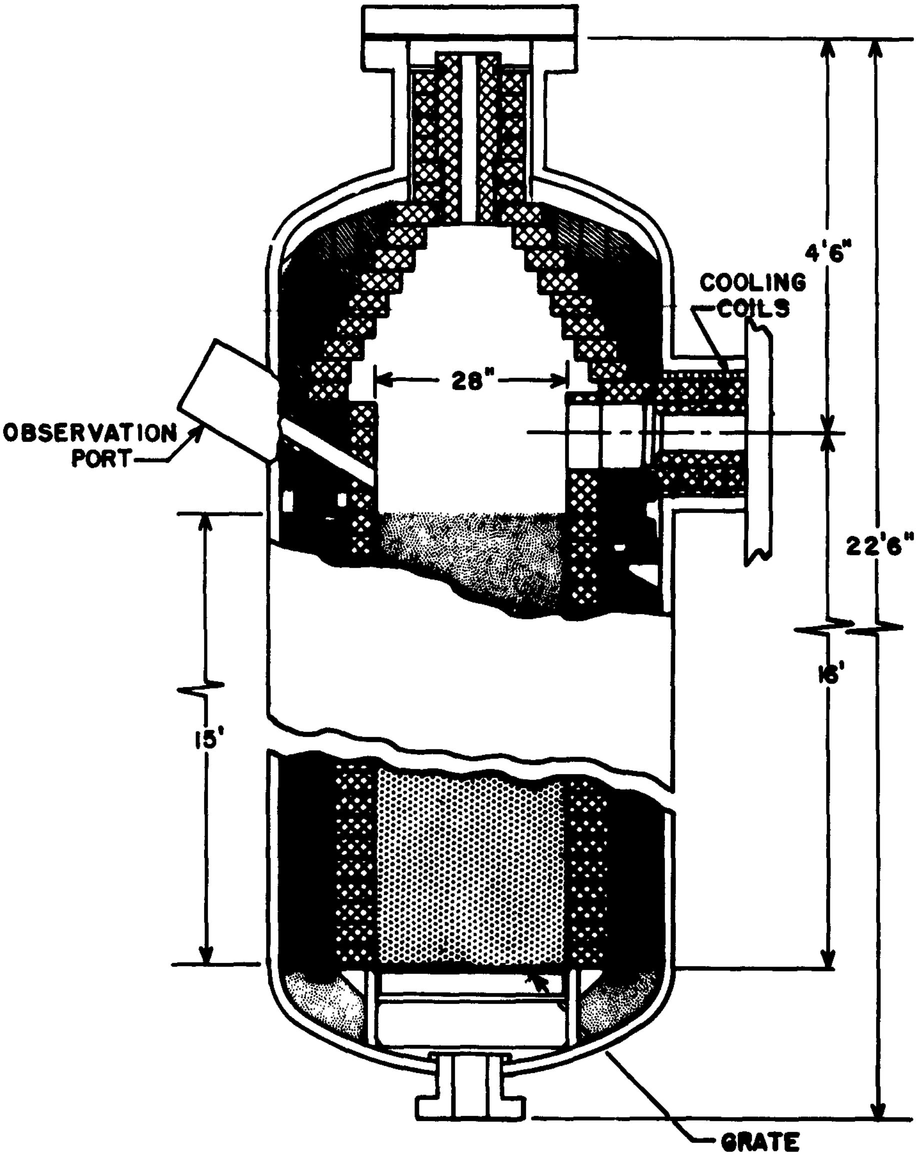

Figure 5. Heater Details

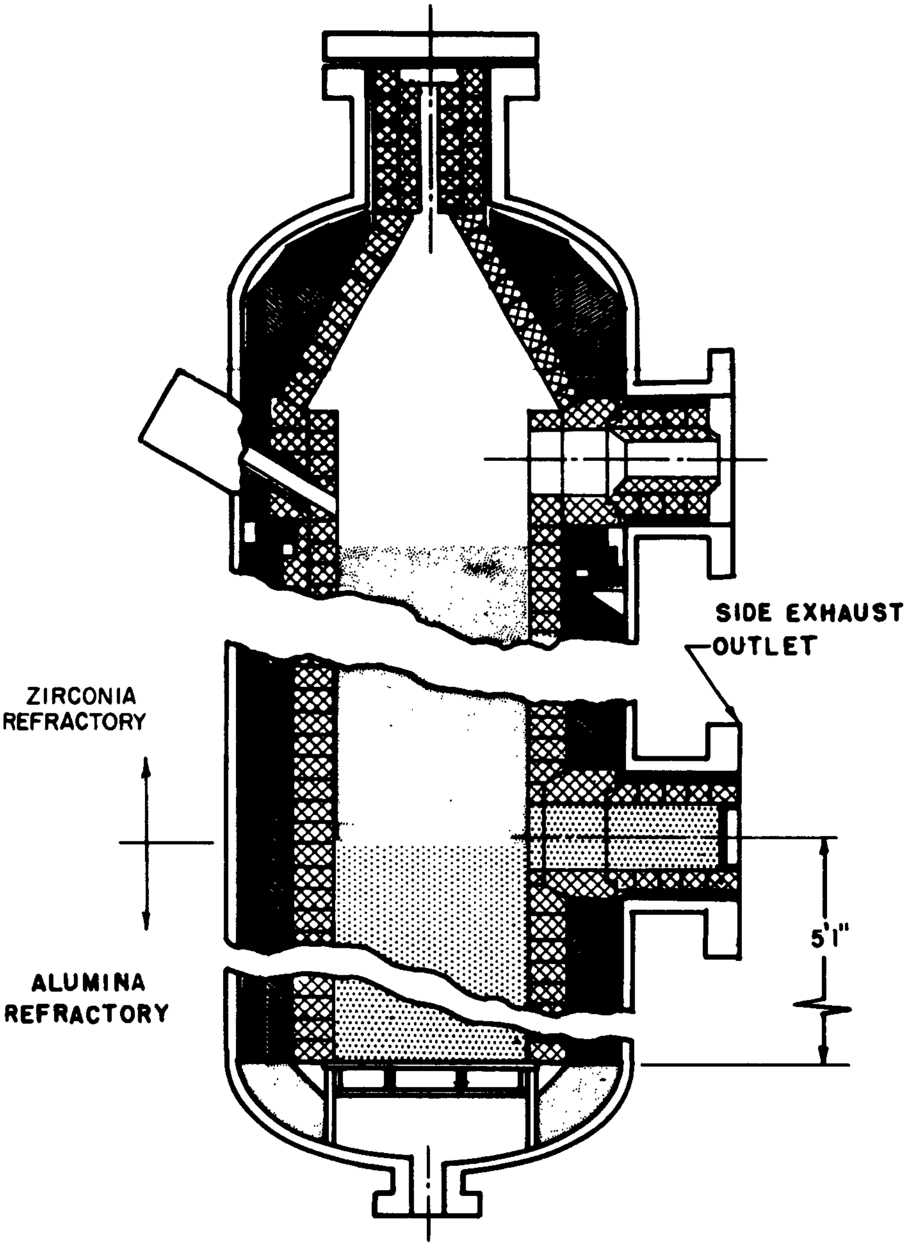

Figure 6. Heater Details (Modified)

TABLE 3 MACH 4 NOZZLE CONTOUR

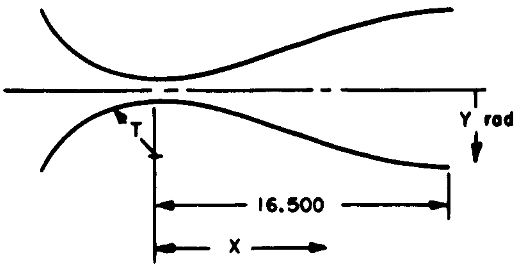

X	Y	X	Y	X	Y
-1.614		0.641	0.679	6.000	1.779
-1.500	1.023	0.736	0.695	6.500	1.839
-1.400	0.968	0.832	0.713	7.000	1.895
-1.300	0.917	0.928	0.732	7.500	1.947
-1.200	0.872	1.025	0.753	8.000	1.996
-1.100	0.830	1.122	0.776	8.500	2.043
-1.000	0.793	1.220	0.799	9.000	2.088
-.0900	0.759	1.318	0.824	9.500	2.131
-0.800	0.730	1.417	0.849	10.000	2.172
-0.700	0.704	1.516	0.876	10.500	2.210
-0.600	0.682	1.615	0.903	11.000	2.246
-0.500	0.663	1.714	0.931	11.500	2.280
-0.400	0.648	1.814	0.959	12.000	2.312
-0.300	0.636	1.914	0.988	12.500	2.342
-0.200	0.628	2.014	1.017	13.000	2.370
0.100	0.623	2.132	1.051	13.500	2.395
0.000	0.621	2.500	1.156	14.000	2.418
0.088	0.622	3.000	1.278	14.500	2.439
0.179	0.626	3.500	1.383	15.000	2.458
0.269	0.632	4.000	1.476	15.500	2.474
0.361	0.641	4.500	1.562	16.000	2.488
0.454	0.651	5.000	1.641	16.500	2.500
0.547	0.664	5.500	1.713		

T = 3.000 rad.

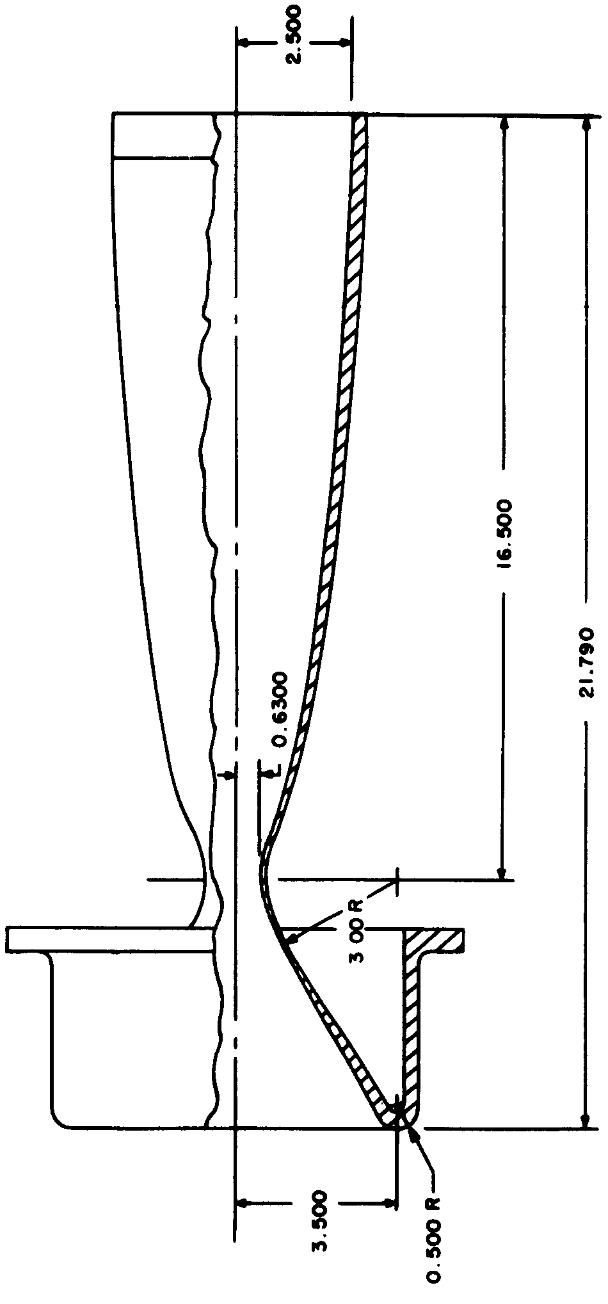

Figure 7. Mach 4 Contoured Nozzle

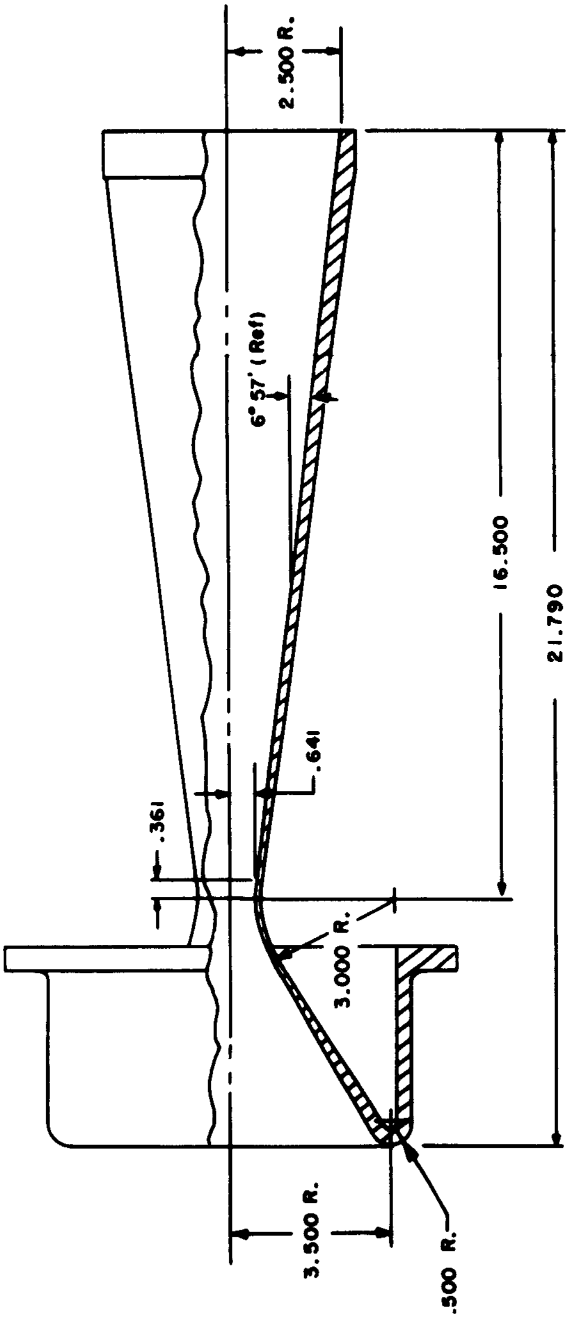

Figure 8. Mach 4 Conical Nozzle

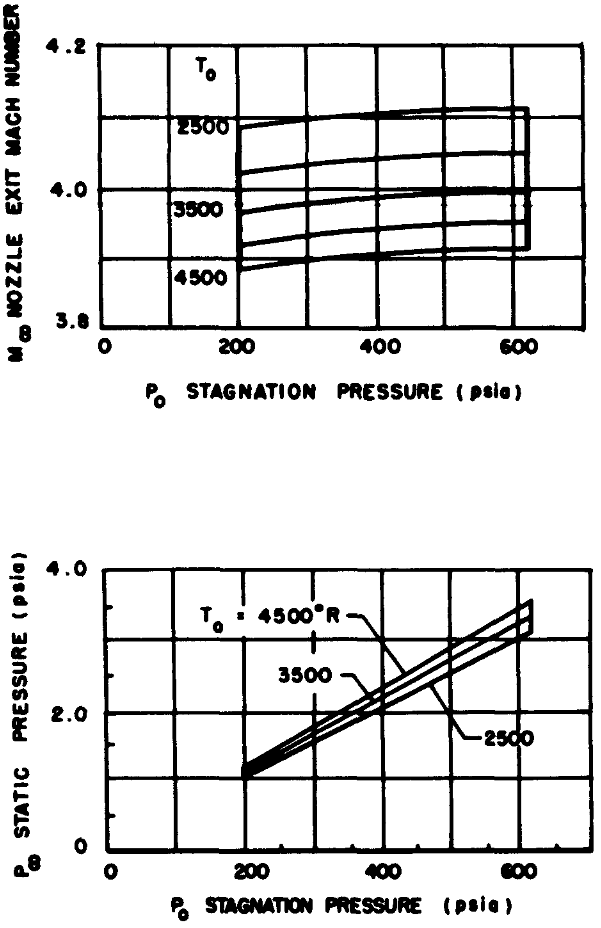

Figure 9. Summary of Theoretical Performance of the High Temperature Facility with the Mach 4 Conical Nozzle

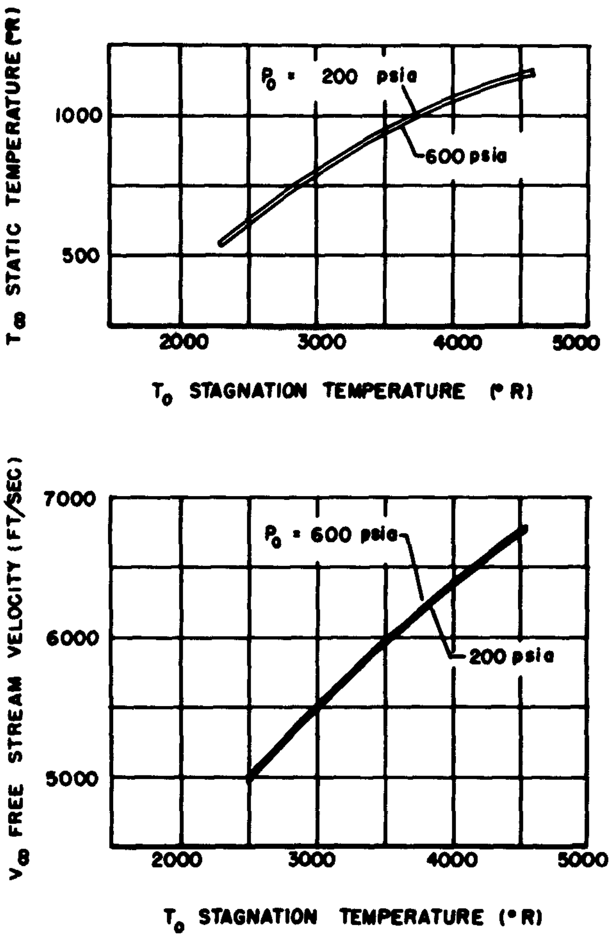

Figure 9. Summary of Theoretical Performance of the High Temperature Facility with the Mach 4 Conical Nozzle

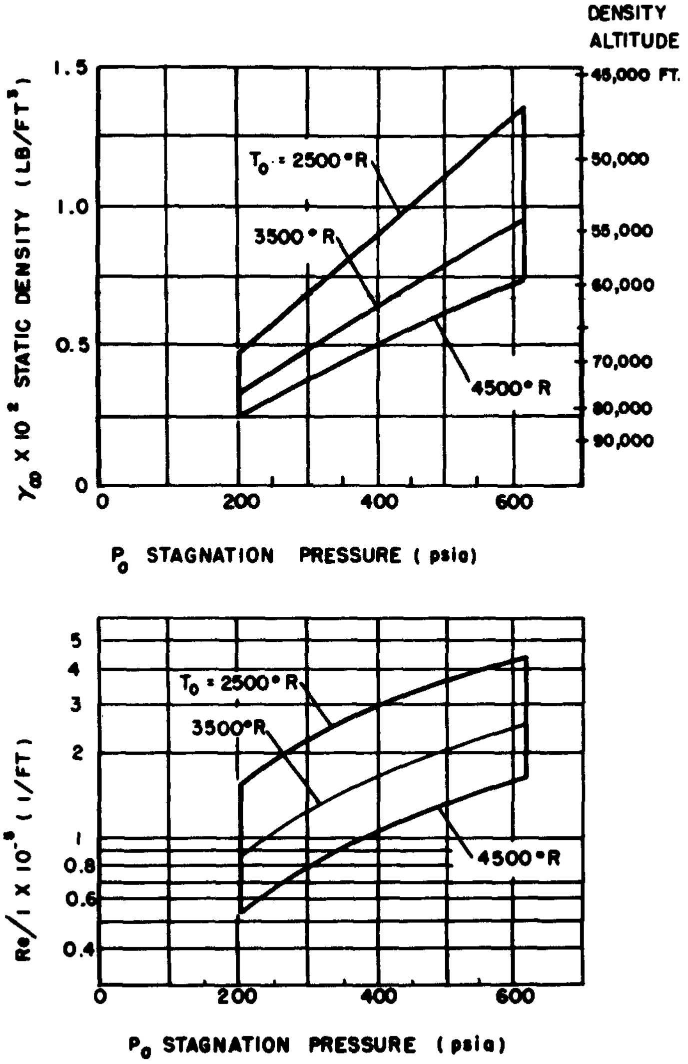

Figure 9. Summary of Theoretical Performance of the High Temperature Facility with the Mach 4 Conical Nozzle

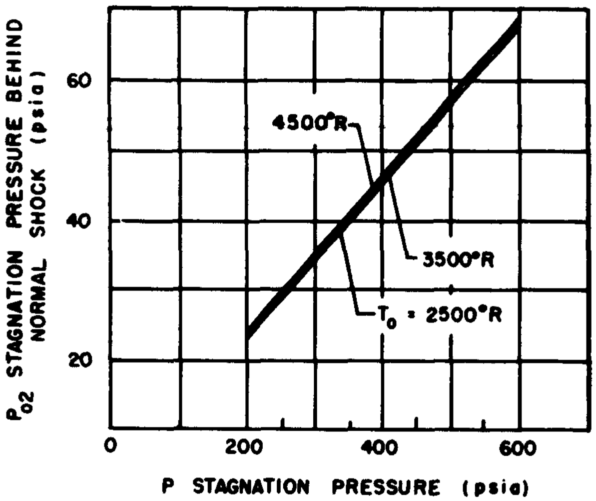

Figure 9. Summary of Theoretical Performance of the High Temperature Facility with the Mach 4 Conical Nozzle

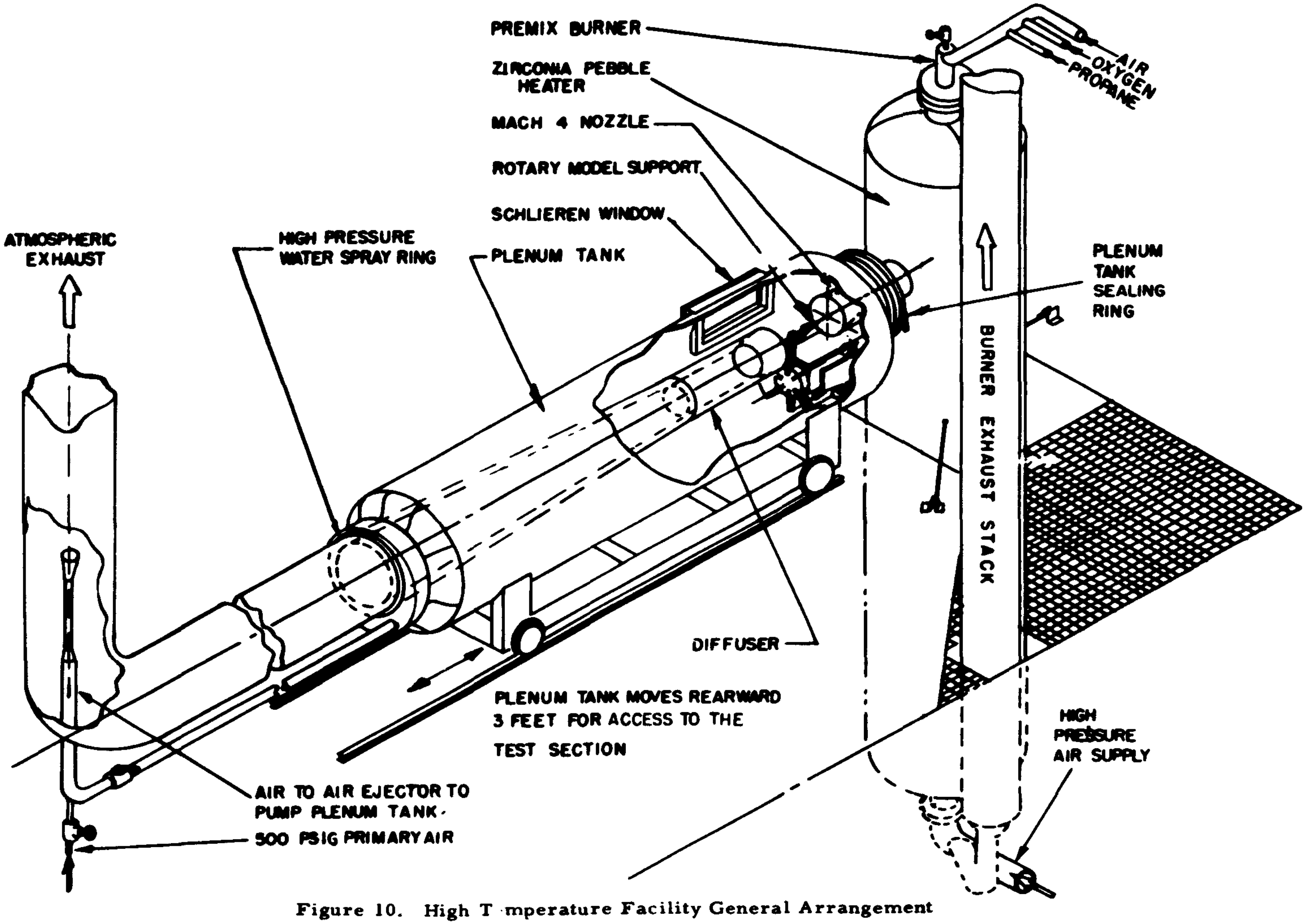

Figure 10. High Temperature Facility General Arrangement

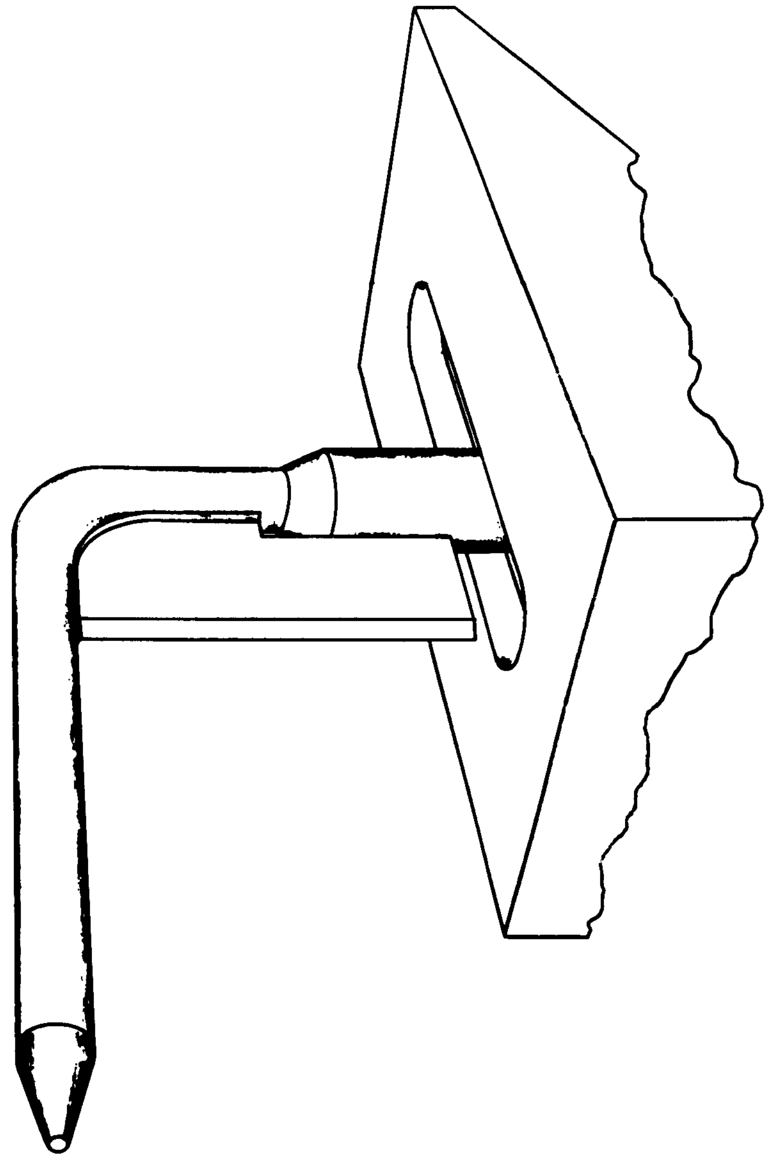

Figure 11. High Temperature Facility Water Cooled Total Head Probe

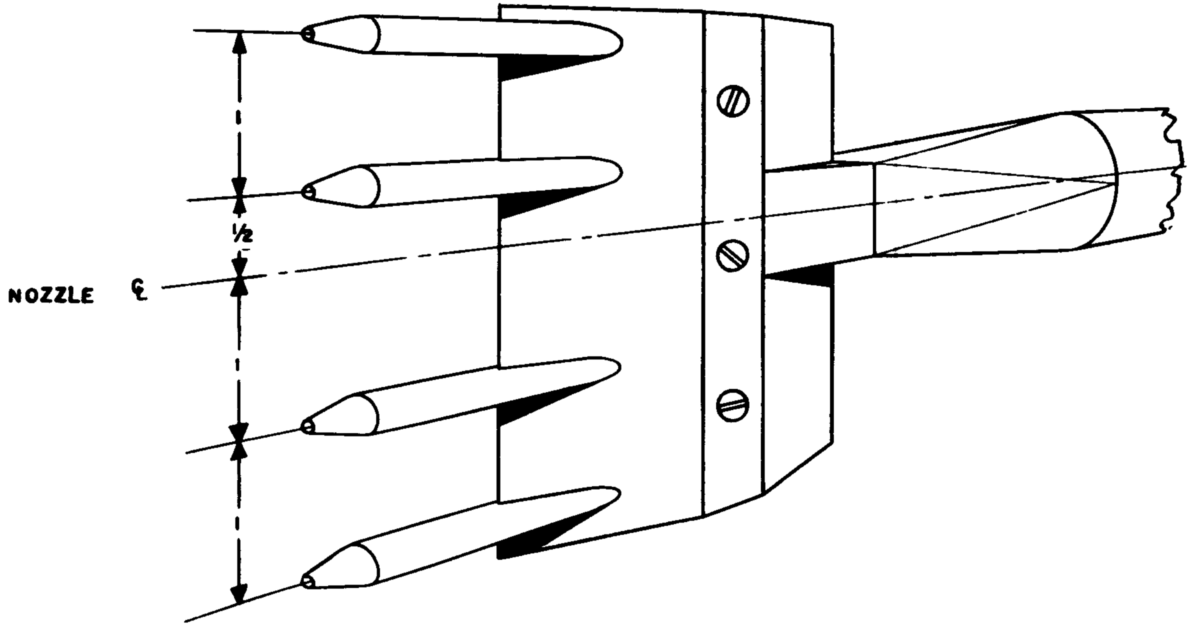

Figure 12. High Temperature Facility Calibration Rake

Aeronautical Systems Division, Directorate of Engineering Test, Deputy for Test and Support, Wright-Patterson AFB, Ohio.
Rpt No. ASD-TDR-63-236. THE HIGH TEMPERATURE HYPERSONIC GASDYNAMICS FACILITY — MACH NUMBER 4 OPERATION. Final report, May 63, 31p. incl illus., tables and refs.

Unclassified Report

The High Temperature, Hypersonic Gasdynamics Facility was developed as a result of the efforts of the Aeronautical Systems Division to extend the state-of-the-art in hypersonic aerodynamics simulation. The High Temperature Facility is an operational hypersonic wind tunnel supplied by high pressure, heated air

(over)

1. Wind Tunnel
2. Hypersonic
3. High Temperature
4. Operation

I. AFSC Project 1426, Task 142601
II. Paul Czysz
III. Aval fr OTS
IV. In ASTIA collection

from a zirconium oxide pebble heater. The maximum stagnation pressure is 40 atmospheres, and the maximum temperature is 4700°R. The facility is one of four of its kind in this hemisphere and the only Air Force facility of its type. This report describes its operation from August 1961 until May 1962 as a Mach 4 aerodynamic test facility. The successful operation of this facility is a significant achievement in the area of hypersonic aerodynamic testing techniques.

Aeronautical Systems Division, Directorate of Engineering Test, Deputy for Test and Support, Wright-Patterson AFB, Ohio.
Rpt No. ASD-TDR-63-236. THE HIGH TEMPERATURE HYPERSONIC GASDYNAMICS FACILITY — MACH NUMBER 4 OPERATION. Final report, May 63, 31p. incl illus., tables and refs.

Unclassified Report

The High Temperature, Hypersonic Gasdynamics Facility was developed as a result of the efforts of the Aeronautical Systems Division to extend the state-of-the-art in hypersonic aerodynamics simulation. The High Temperature Facility is an operational hypersonic wind tunnel supplied by high pressure, heated air

(over)

1. Wind Tunnel
2. Hypersonic
3. High Temperature
4. Operation

I. AFSC Project 1426, Task 142601
II. Paul Czysz
III. Aval fr OTS
IV. In ASTIA collection

from a zirconium oxide pebble heater. The maximum stagnation pressure is 40 atmospheres, and the maximum temperature is 4700°R. The facility is one of four of its kind in this hemisphere and the only Air Force facility of its type. This report describes its operation from August 1961 until May 1962 as a Mach 4 aerodynamic test facility. The successful operation of this facility is a significant achievement in the area of hypersonic aerodynamic testing techniques.

Aeronautical Systems Division, Directorate of Engineering Test, Deputy for Test and Support, Wright-Patterson AFB, Ohio.
Rpt No. ASD-TDR-63-236. THE HIGH TEMPERATURE HYPERSONIC GASDYNAMICS FACILITY — MACH NUMBER 4 OPERATION. Final report, May 63, 31p. incl illus., tables and refs.

Unclassified Report

The High Temperature, Hypersonic Gasdynamics Facility was developed as a result of the efforts of the Aeronautical Systems Division to extend the state-of-the-art in hypersonic aerodynamics simulation. The High Temperature Facility is an operational hypersonic wind tunnel *supplied by high pressure, heated air*

(over)

1. Wind Tunnel
2. Hypersonic
3. High Temperature
4. Operation

I. AFSC Project 1426, Task 142601
II. Paul Czysz
III. Aval fr OTS
IV. In ASTIA collection

from a zirconium oxide pebble heater. The maximum stagnation pressure is 40 atmospheres, and the maximum temperature is 4700°R. The facility is one of four of its kind in this hemisphere and the only Air Force facility of its type. This report describes its operation from August 1961 until May 1962 as a Mach 4 aerodynamic test facility. The successful operation of this facility is a significant achievement in the area of hypersonic aerodynamic testing techniques.

Aeronautical Systems Division, Directorate of Engineering Test, Deputy for Test and Support, Wright-Patterson AFB, Ohio.
Rpt No. ASD-TDR-63-236. THE HIGH TEMPERATURE HYPERSONIC GASDYNAMICS FACILITY — MACH NUMBER 4 OPERATION. Final report, May 63, 31p. incl illus., tables and refs.

Unclassified Report

The High Temperature, Hypersonic Gasdynamics Facility was developed as a result of the efforts of the Aeronautical Systems Division to extend the state-of-the-art in hypersonic aerodynamics simulation. The High Temperature Facility is an operational hypersonic wind tunnel *supplied by high pressure, heated air*

(over)

1. Wind Tunnel
2. Hypersonic
3. High Temperature
4. Operation

I. AFSC Project 1426, Task 142601
II. Paul Czysz
III. Aval fr OTS
IV. In ASTIA collection

from a zirconium oxide pebble heater. The maximum stagnation pressure is 40 atmospheres, and the maximum temperature is 4700°R. The facility is one of four of its kind in this hemisphere and the only Air Force facility of its type. This report describes its operation from August 1961 until May 1962 as a Mach 4 aerodynamic test facility. The successful operation of this facility is a significant achievement in the area of hypersonic aerodynamic testing techniques.